S. Cerro, R. Galindo*, M. Llusar*, J. Badenes*, G. Monrós**

Photocatalytic Glazed Tiles

THE AUTHOR

Dr. Sara Cerro earned her PhD in Inorganic Chemistry at Jaume I University, Castellón (Spain). **E-Mail: monros@uji.es**

ABSTRACT

A parent glass in the SiO_2–CaO–ZnO–B_2O_3–K_2O–Al_2O_3 system, deposited and processed by the monoporosa firing method (1085 °C), was coated using a sol–gel procedure and by serigraphy with silica, bismuth oxide, zirconia, and anatase with thermal treatment at 600 °C. The photocatalytic activity of the samples determined by degradation in the Orange II dye test shows that a first-order reaction according to the Langmuir-Hinshelwood model is followed. From the UV-Vis-NIR results the band gap calculated is around 3.5 eV for the parent glass and that with a silica coating, and slightly lower for the other coatings. The needle-shaped microstructure of the parent glass shows the best photocatalytic results in agreement with the literature. The preserved zircon microstructure can explain the relatively high results for the silica coating, which unexpectedly showed better results than both the anatase and tetragonal zirconia coatings. Finally, the interaction with the parent glass can explain the relatively high results of the bismuth oxide sample

KEYWORDS

tile coating, photocatalysis, glass ceramic, orange II

Interceram 61 (2012) [5]

1 Introduction

Advanced oxidation processes (AOPs) are based on sufficient concentrations of hydroxyl radicals to degrade dissolved organic compounds present in water or those that are dispersed in air to mineral forms or at least to harmless organic compounds. The OH radical is the most important natural oxidant in tropospheric chemistry [1]. It is often termed the "detergent" of the atmosphere, as it reacts with many pollutants, initiating their cleaning process, while it also plays an important role in the elimination of greenhouse gases such as methane or ozone. The features that make AOPs attractive are, among others, that they break up the pollutant, which is not concentrated or transferred to another medium, providing complete or almost complete mineralization of the organic pollutants, and that they can serve in breaking up the vast majority of organic compounds, especially non-biodegradable compounds such as organochlorated compounds, PCBs, PAHs, etc. It is a safe and clean technology and, in certain processes, solar radiation can be used as process initiator.

Titanium oxide is currently the photocatalyst reference material, given its high activity, relative stability, low cost, and low toxicity. However, certain problems need to be addressed such as the low velocity of photocatalysis, generation of toxic degradation intermediates, deactivation of the material, and need for UV irradiation as its band gap does not match that of sunlight: the use of ceramic composites could enhance these aspects [2]. Conversely, recent reports have shown that nanostructured anatase exhibits higher activity and selectivity than commercially available TiO_2 catalysts (Degussa P25). These favourable characteristics are related to the small size of the crystallites, which defines the surface area available for adsorption and decomposition of organic pollutants. The higher surface-to-bulk ratio of these ultrafine particles could favour the transfer of photogenerated charge carriers (i.e. e^- and h^+) to the adsorbed molecules. However, when the size of a semiconductor decreases to an extent that the relative proportion of surface and bulk regions are comparable, the band structure becomes discrete, and its chemical and optical properties differ from those of the bulk material. This phenomenon is known as the quantum size effect (QSE), and its existence in nanometre-sized TiO_2 particles is controversial. Thus, Serpone et al. proposed that this effect is not perceptible for particles larger than 2 nm, whereas other authors have attributed the noticeable shifts in the electronic spectra of TiO_2 with particle sizes smaller than 10 nm to the QSE [3].

Thin semiconductor film coatings can be obtained by serigraphy deposition of appropriate inks on a glazed tile that is fired up to 600 °C in order to establish nanostructured semiconductor particles due to its higher surface-to-bulk ratio favouring the transfer of photogenerated charge carriers. This paper presents examples of the use of ceramic glazed tiles coated with nanostructured SiO_2, TiO_2, ZrO_2, and Bi_2O_3 in the treatment of wastewaters using Orange II as the target [4].

* Unidad de Química Inorgánica Medioambiental y Materiales Cerámicos, Dpto. Química Inorgánica y Orgánica, Universidad Jaume I, Castellón (Spain)

2 Experimental

The inks were prepared by sol-gel dispersion of salt precursors of SiO_2, TiO_2, ZrO_2, and Bi_2O_3 (TEOS, titanium isopropoxide, zirconium acetate, and bismuth nitrate pentahydrate, respectively). The inks were deposited on a monoporosa glazed tile (1085 °C) by serigraphy using a 120-thread screen. The resulting films were fired at 600 °C with a thermal cycle of 50 min with 15 min of soaking time at 600 °C. The monoporosa glaze used in this work is a glass in the SiO_2–CaO–ZnO–B_2O_3–K_2O–Al_2O_3 system that has a relatively high photoactivity [3].

The resulting coated tiles (Fig. 1 a) were characterized by the low-glancing-angle X-ray diffraction (XRD) method, UV-Vis-NIR spectroscopy using the diffuse reflectance technique, and scanning electron microscopy (SEM).

Low-glancing-angle X-ray diffraction GID (glancing incidence diffraction) method XRD patterns were obtained with a Siemens D-500 diffractometer using Ni-filtered Cu-K_α radiation between 10 and 70 °. Maintaining a low-incidence angle throughout the scan increases the path length through the sample and decreases the X-ray penetration depth, resulting overall in diffraction patterns with higher relative sample peak intensities and lower substrate scatter [4].

UV-Vis-NIR spectroscopy using the diffuse reflectance technique was carried out with a Perkin-Elmer (Lambda 2000) spectrophotometer in the range 200–800 nm in order to obtain the band gap of the catalyst from the absorption threshold wavelength.

The microstructure of representative fired samples was studied by SEM, using a Leo-440 Leyca electron microscope equipped

with an Energy Dispersion X-ray (EDX) attachment by Oxford University (work conditions: 10–20 kV acceleration voltage and a probe intensity of 150–500 pA). The EDX analysis was obtained at relatively low magnification as an average of the area of the image on the scanning electron microscope screen. Samples were graphite coated by a sputtering procedure before SEM-EDX studies.

The photocatalytic tests were carried out using a cylindrical reactor (Fig. 1 b) 22 cm in height and 14 cm in diameter with walls coated with glazed ceramic pieces around 14 cm high and 4 cm width. The reactor containeda solution of $0.6 \cdot 10^{-5}$ M Orange II in a controlled neutral pH, avoiding buffer addition. The $0.6 \cdot 10^{-5}$ M solution of monoazo dye at pH 7 was analyzed by UV-Vis-NIR to determine the appropriate wavelength for measurement of the remaining Orange II dye. The results indicate that λ = 485 nm was the maximum of absorbance. The UV irradiation source was a 125-W mercury lamp emitting in the range 254–365 nm. The lamp was placed in a refrigerated quartz tube (28 cm high and 5 cm in diameter) surrounded by a coaxial tube, also made of quartz, 28 cm high and 6.5 cm in diameter, across which circulates a refrigerated current of water. The estimated power surface density of the emitting UV light was 0.1 W/cm^2. The tube was placed into the cylindrical reactor (20 cm high and 14 cm diameter) containing 750 ml of an irradiated solution of Orange II. The suspension was first stirred in the dark for 15 min to reach equilibrium sorption of the dye. An aliquot of samples was taken every 15 min to measure the remaining dye concentration by spectroscopy at the maximum of absorbance.

Specular reflectance (SR) at 650 nm and the average roughness (R_a) of the tile surface were measured using an X-Rite SP60 reflectometer and an ASM3 roughness tester, respectively. The measurements for the parent glass were SR = 3.6 % and R_a = 0.05 µm.

Blank experiments with Orange II solution without catalyst addition, were conducted before the photocatalytic experiments. Likewise commercial anatase P25 supplied by Degussa was used as a reference to compare its photocatalytic activity with the prepared samples.

3 Results and discussion

3.1 XRD characterization of glazed tiles

Low-glancing-angle X-ray diffraction GID patterns of prepared samples are shown in Fig. 2. The parent glaze crystallizes zircon and low intense peaks associated with tetragonal zirconia were also detected. The silica coating doesn't show any crystallization associated with SiO_2, the bismuth film shows a weak crystallization associated with Bi_2O_3 and a strong crystallization of an unidentified phase X. In the case of the titanium film anatase crystallizes, and finally for the zirconium film tetragonal zirconia crystallizes and considerably increases its intensity peaks.

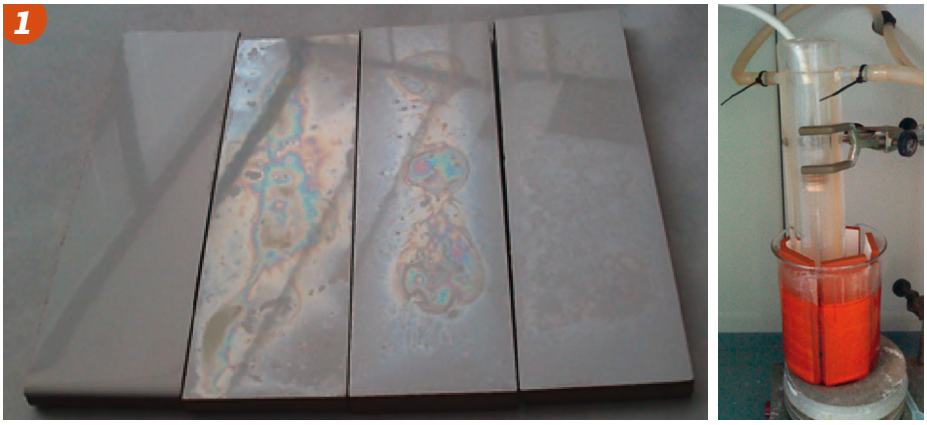

Fig. 1 • Glazed samples (left) and reactor view (right)

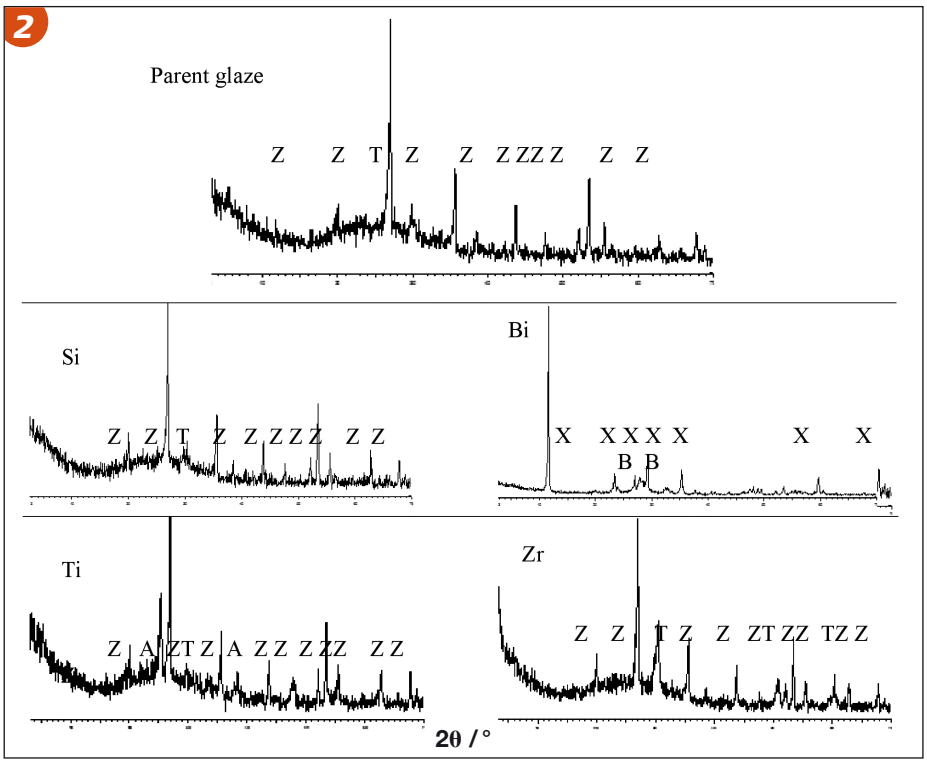

Fig. 2 • Low-glancing-angle X-ray diffraction GID patterns of the samples. Crystalline phases: Z – $ZrSiO_4$, T – Tetragonal zirconia ZrO_2, B – Bi_2O_3, A – Anatase, X – unidentified phase

3.2 UV-Vis-NIR spectroscopy

The UV-Vis-NIR spectra (Fig. 3) are dominated in all cases by a broad peak associated with metal–ligand charge transfer ($M^{n+} \leftrightarrow O^{2-}$). From the threshold value of absorbance the band gap calculated for the Si sample is 3.5 eV, and the value shifts to slightly lower band gaps in the sequence Zr (3.4), Ti (3.3), and Bi (3.2 eV).

3.3 SEM microstructure

Figure 4 shows the microstructure of representative glazed samples fired at 600 °C and their EDX mapping analysis. The EDX mapping analysis shows 1-µm radius particles in the parent glass that are associated with ZrO_2 crystallization, and also needle-shaped particles in the parent glass around 1 mm long associated with $ZrSiO_4$ crystallization. The Si-glazed sample is similar to the parent glass microstructure with irregularly shaped ZrO_2 and needles of zircon crystallization, but the major intensity of Si in the mapping analysis indicates the presence of a silica film coating the surface. In the case of the Ti sample an anatase film is clearly observed in some cracks on the surface.

The surface roughness (Table 1) is similar in all samples, including the parent glass (R_a =

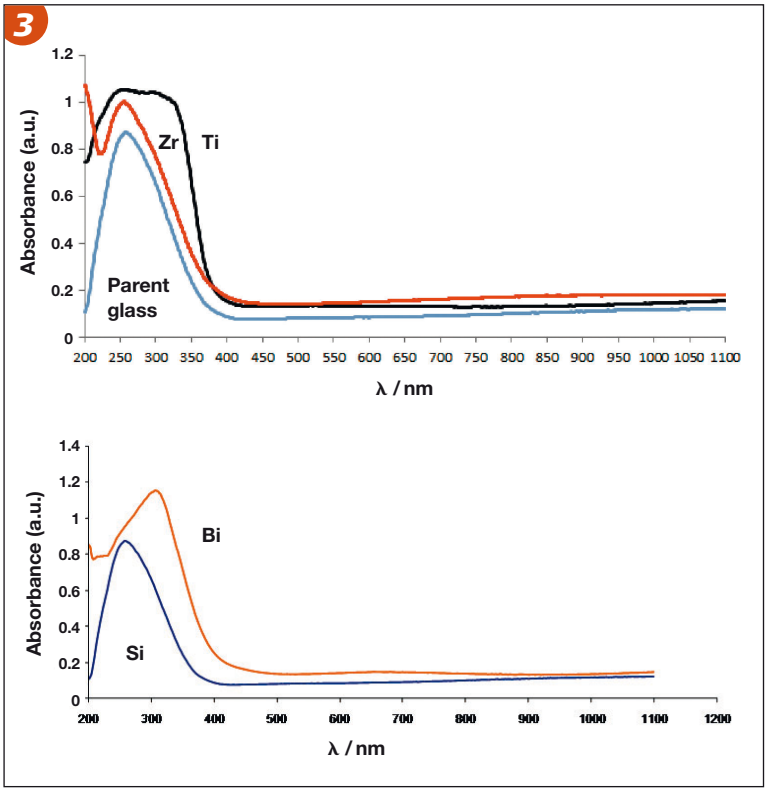

Fig. 3 • UV-Vis spectra of coated tiles at 600 °C/1h

ca. 0.05 μm). The specular reflectance (Fig. 1, left) and Table 1) is very low for both the parent glass and Si sample (3.8 %), increases in the Zr and Bi samples (8.3 and 12.8 %, respectively) and shows relatively high reflectance for the Ti sample (20.5 %).

3.4 Photocatalytic test

The test of photocatalytic activity for the samples was carried out following the above-mentioned experimental procedure. The change of dye concentration versus time of irradiation is plotted in Fig. 5. The obtained results indicate a linear degradation curve for the Orange II solution in the "blank" test carried out without catalyst. This linear behaviour is in agreement with the direct photolysis effect of UV irradiation in the absence of a catalyst. The presence of a catalyst leads to a decay of the dye concentration due to its photocatalytic capacity.

The decay of the dye concentration upon photocatalytic oxidation of different dyes fitted the Langmuir-Hinshelwood (L-H) kinetics model [4–8]. When the initial con-

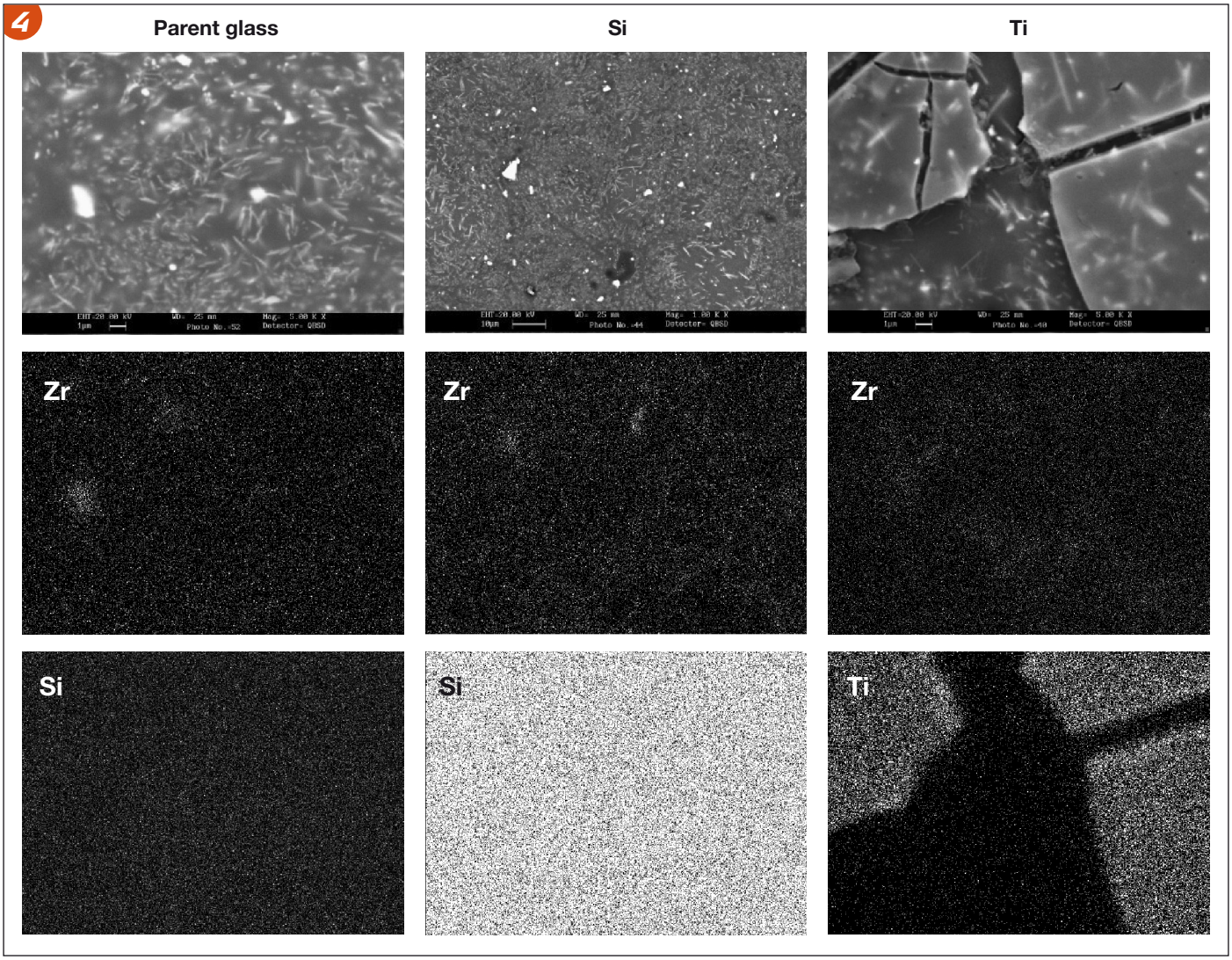

Fig. 4 • Microstructure of parent glass and representative coated samples fired at 600 °C and its EDX mappings

centration (C_o) and the adsorption are low, the kinetic model follows the equation:

$$\ln\frac{c}{c_0} = kKt = K_{app}t$$

where
t – illumination time
C – actual dye concentration.
A plot of $\ln(C/C_o)$ versus time of data fitting the L-H model shows a linear adjustment and the slope of the linear regression is the apparent first-order rate constant K_{app}. The half life ($t_{1/2}$) can be calculated with the following expressions:

$$\ln\frac{c_0/2}{c_0} = K_{app}t_{1/2} \qquad t_{1/2} = -\frac{\ln 2}{K_{app}}$$

Plots of $\ln(C/C_o)$ versus time of irradiation are in agreement with the L-H model because the lineal behaviour of each curve indicates that a first-order reaction is taking place during Orange II degradation. The kinetics parameters of the photocatalytic reaction $t_{1/2}$ and the square of the correlation coefficient R^2 calculated from the above equations can be seen in Table 1 indicating a goodness-of-fit measure.
In order to obtain powders with a high catalyst capacity it is necessary to simultaneously have two apparently contradictory properties: a high specific surface area in order to adsorb substrates and a high crystallinity (or less surface and bulk defects) to diminish the electron-hole recombination. From the obtained results, the best photocatalytic results (lowest $t_{1/2}$) are seen with silica deposition, bismuth oxide deposition shows a similar value, and zirconia and titania coatings show inferior results.
The photocatalytic activity observed is high in spite of the low surface interaction of the catalytic surface of the glazed tiles (only 0.03 m^2). The preserved zircon microstructure can explain the relatively high results for silica, which unexpectedly shows better results than anatase or tetragonal zirconia coatings. In effect the parent glass shows the best photocatalytic results ($t_{1/2}$ = 103 min) in agreement with the literature [2, 7, 8] in the sense that the needled-shaped zircon surface crystallizations show relatively high photoactivity. Finally, the interaction with the parent glass can explain the relatively high results of the bismuth oxide sample.

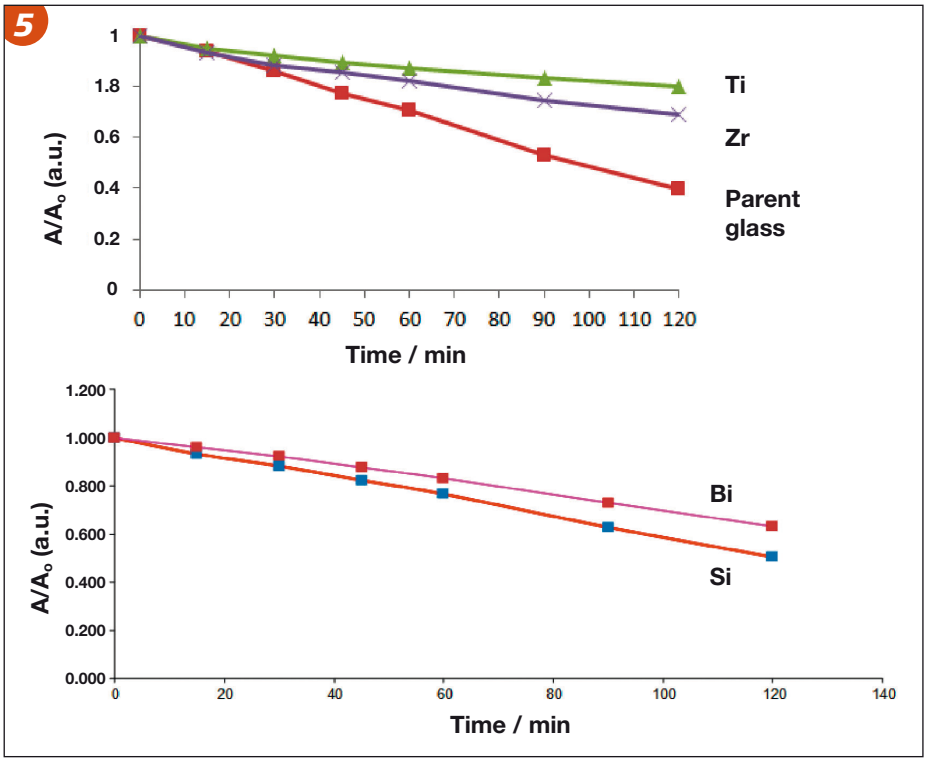

Fig. 3 • UV-Vis spectra of coated tiles at 600 °C/1h

4 Conclusions

A parent glass in the SiO_2–CaO–ZnO–B_2O_3–K_2O–Al_2O_3 system, deposited and processed by the monoporosa firing method (1085 °C), was coated using a sol–gel procedure and by serigraphy with silica, bismuth oxide, zirconia, and anatase. The photocatalytic activity of the samples determined by degradation in the Orange II dye test shows that a first-order reaction according to the Langmuir-Hinshelwood model is followed. From the UV-Vis-NIR results the band gap calculated is around 3.5 eV for the parent glass and that with a silica coating, and slightly lower for the other coatings. The needle-shaped microstructure of the parent glass shows the best photocatalytic results in agreement with the literature. The preserved zircon microstructure can explain the relatively high results for the silica coating, which unexpectedly showed better results than the anatase or tetragonal zirconia coatings. Finally, the interaction with the parent glass can explain the relatively high results of the bismuth oxide sample

Table 1 • Photocatalytic and surface data of samples

Sample	pH (initial)	pH (final)	E_g / eV	$t_{1/2}$ / min	R^2	SR / % (650 nm)	R_a / µm
Without	7.5	7.5	–	1208	0.922	–	–
P25	7.5	7.6	–	38	0.933	–	–
Parent glass	7.6	6.4	3.5	103	0.984	3.6	0.05
Si	7	6.7	3.5	123	0.9842	3.8	0.05
Bi	7.4	7.3	3.2	182	0.9871	12.8	0.05
Ti	7.6	7.7	3.3	392	0.971	20.5	0.06
Zr	7.6	7.2	3.4	228	0.994	8.3	0.06

Acknowledgments

The authors acknowledge the financial support given by the FUNDACION CAJA CASTELLÓN-UJI, P1-1B2010-09 project.

References

[1] **Isaksen, I.S.A., Dalsøren, S.B.:** Getting a better estimate of an atmospheric radical. Science **331** (2011) 31–39
[2] **Gargori, C., Galindo, R., Llusar, M., Tena, M.A., Monrós, G., Badenes, J.A.:** Photocatalytic degradation of Orange II by titania addition to sol-gel glasses. J. of Sol-Gel Sci. and Tech. **50** (2009) 314–320
[3] **Coronado, J.M., Maira, A.J., Conesa, J.C., Yeung, K.Y., Augugliaro, V., Soria, J.:** EPR Study of the Surface Characteristics of Nanostructured TiO_2 under UV Irradiation, Langmuir (2001), 17, 5368–5374
[4] **Ozalas, K., Hajek, B.F.:** X-ray diffraction analysis of thin clay films from dilute suspensions using glancing incidence diffraction. Clays and Clay Minerals **44** (1996) [6] 817
[5] **Galindo, R.:** Vidriados cerámicos Fotoactivos, Tesis Doctoral, Universitat Jaume I, Noviembre (2008)
[6] **Konstantyinou, I.K., Albanis, T.A.:** TiO_2-assisted photocatalytic degradation of azo dyes in aqueous solution: kinetic and mechanistic investigations. A review, App. Catalyst B: Environmental **49** (2004)1–14
[7] **Ruiz, O., Sanmiguel, F., Gargori, C., Galindo, F., Monrós, G.:** Estudio de la capacidad de degradación fotocatalítica de vidriados cerámicos. QUALICER 2008, ISBN 978-84-95931-37-5, PBC15-33, (2008)
[8] **Meseguer, S., Galindo, F., Sorlí, S., Gargori, C., Tena, M.A., Monrós, G.:** Vidriados cerámicos con actividad fotoquímica: aplicación potencial a depuración ambiental. Cerámica Información **333** (2006) 61–68

Received: 25.06.2012